Computational Electromagnetics for the Evaluation of EMC Issues in Multi-Component Energy Systems

M. R. Barzegaran and O. A. Mohammed

Energy Systems Research Laboratory, Department of Electrical and Computer Engineering
Florida International University, Miami, FL 33174, USA
mohammed@fiu.edu

Abstract — This paper reviews the physics based modeling based on the electromagnetic stray fields and interference in the electric power network. The low frequency as well as high frequency equivalent source modeling of the power components for the study of radiated and conducted electromagnetic compatibility were implemented. The 3-D finite element analysis with some modification were applied in the solution method, as well as meshing strategies for the simulation of large scale components. Moreover, the stray field of the components was utilized for improving the control of the machine-drive system using hardware in loop method. The optimization in the design of the components such as the power converter based on the EMC compliance was also applied. This was achieved by coupling MATLAB with 3-D finite element technique for applying the numerical optimization techniques. The results were verified experimentally.

Index Terms — EMC compliance, equivalent source modeling, large scale computational problems, low frequency and high frequency modeling.

I. INTRODUCTION

The compliance with Electromagnetic Compatibility (EMC) standards is an increasingly important aspect in the design of practical engineering systems. Consideration of EMC issues at the design stage is necessary to ensure the functional safety and reliability of complex modern products, which are increasingly reliant on electronic sub-systems to provide power, communications, control and monitoring functions that are needed to provide enhanced levels of functionality of systems. Typical examples include transportation vehicles (road, rail, sea and air), manufacturing plants, power generation and distribution, and communications. The opportunities for using numerical simulation techniques to predict and analyze the system EMC and related issues (e.g., human field exposure and installed antenna performance) are therefore of considerable interest in many industries.

A basic performance of modern electrical power systems is significantly related to the area of low frequency disturbances. Based on the above background, the importance of low frequency EMC study is considerably increasing. On the other hand, power electronic technologies are also used in evolving machine-drive equipment such as vessels and aircrafts. The magnetic signature is observable in the low frequency local magnetic field, but then several threats are present in military applications: detection and classification by and subsequent detonation of sea mines, detection and localization of submarines out of the air. Due to the improvement of the sensitivity of electromagnetic field sensors and smart signal processing techniques, signature reduction is vital. Thus, the first goal is to decrease the detection range by complying with the strict signature requirements.

The other signature study aspect of the radiated fields in low frequency is condition monitoring of the components. The faults in the winding of the machines as well as switch failures and many other problems can be detected without the need to dismantle the system. This is critically beneficial for the sensitive applications in which it may not be easily possible to get near to the components for online testing, and on the other

Submitted On: July 17, 2014
Accepted On: September 5, 2014

hand offline testing of the component is costly.

The previous works in the study of the radiated fields in power system can be categorized into EMC studies in power systems, electromagnetic computational modeling studies, electromagnetic signature studies, system monitoring studies and fault and failure diagnosis. The electromagnetic computational modeling is the concern of this paper.

The modeling process in the field of electromagnetic compatibility means the establishment of a connection between the source of interference or any other cause and its effect, which can be the response of the component as the part of the system. This relationship can be established in several ways depending on the type of problem, its complexity, and the degree of approximations with respect to an exact formulation. The possible methods involve:

- Using circuit theory for describing the conducted disturbance, such as voltage dips, over-voltages, voltage stoppages, harmonics, and common ground coupling [1], [2].
- Using an equivalent model (usually circuit) with either distributed or lumped parameters, such as in low-frequency electromagnetic field coupling expressed in terms of mutual inductances and stray capacitances, field-to-line coupling using the transmission line approximation, and cable crosstalk [3], [4].
- Formulating the problem in terms of formal solutions to Maxwell's equation and making analytical models based on that [5].
- Physics based modeling using numerical methods such as finite element method, finite differential method, method of moments and so forth [6]-[8].

Generally, the methods used in EMC modeling are not only to visualize electromagnetic phenomena, but also to predict and suppress the interferences.

In this paper, first the procedure of physics based modeling for EMC study is explained. Then, the equivalent source modeling versus 3-D full finite element modeling is discussed. Afterward, the EMC modeling of the power converter with the purpose of the optimization of power electronic components' performance is described. Through these studies, the techniques for the physics based modeling for special purpose are discussed.

II. PHYSICS BASED MODELING FOR THE ANALYSIS OF MACHINE DRIVE

A. Multi-scale problems

In applications such as radiated emissions or immunity of a system, cables and any ground loop current and on-board antennas can be considered as a complex multi-port antenna that can be characterized using electromagnetic modeling techniques. For building an EMC model, however, it is necessary to consider a range of modeling techniques, as outlined in Table 1, operating at a number of different levels. The clearest need for combining models of different types is the integration of circuit behavior ("type A3" models) with the electromagnetic performance of the installation (a "type A1" model). However, difficulties in prediction of EMI still exist. As the number of components within a device increase, the complexity in modeling all the parasitic, especially the mutual coupling ones, would increase exponentially, resulting in a task that is unpractical even with today's most powerful computers. Therefore, in some cases a combination of the models type A2 and A3 may be useful for computationally expensive calculation. Moreover, the complexity of parameter extraction can be reduced by only modeling of the major EMI related components and circuits. Ideally, such a simplification would need some specialist knowledge of the device electrical behavior and basic EMI characteristics. For example, a distinction between the power handling and logic circuits in a motor drive will justify the concentration on salient EMI related circuitry and components, thus, leading to considerably reduced efforts in parameter extraction.

Due to the nature of the multi-scale problem, which is the multi-level numerical modeling, as well as the requirement of the numerical test environment which needs to be simple and quickly recreated, the separate modeling of each of the components and sub-components is needed. Therefore, it is beneficial to divide the problem

into three levels, as shown in Fig. 1.

The device level consists of each of the physical model of all components calculated from a 2D or 3D quasi-static electromagnetic finite element analysis. In the device level, the component models can be divided into several subsystems, based upon their power range, their location inside the components, their degree of importance from EMC and EMI issues, force outage rate, and the related fault diagnosis issues. The interface level consists of any resistive, capacitive, or inductive paths between enclosures of the components and the additional decoupling capacitor which are used to reduce the area of ground current loop and also to cut the current path and prevent it to enter the control units. The environmental level consists of the physical model of chamber filled with air and the enclosure model of each of the components placed in it.

Table 1: Classification of the numerical level necessary to predict the different performance measures in the virtual test environment

	Model Dimension	Model Character	Objectives
A1	3D in time or Frequency Domain	Electromagnetic (surface or volumes meshing)	3D electromagnetic field distribution and related parameters
A2	2D or 3D quasi-static analysis in time harmonic domain	Quasistatic, electromagnetic (surface, volumes, or peripheral meshing)	Calculation of low to high frequency RLC elements of each of the components, frames, and frame to outer chamber
A4	0D in time or frequency domain	Lumped element circuit (discrete mathematical models)	Physics-based circuit model (circuit simulation environment)

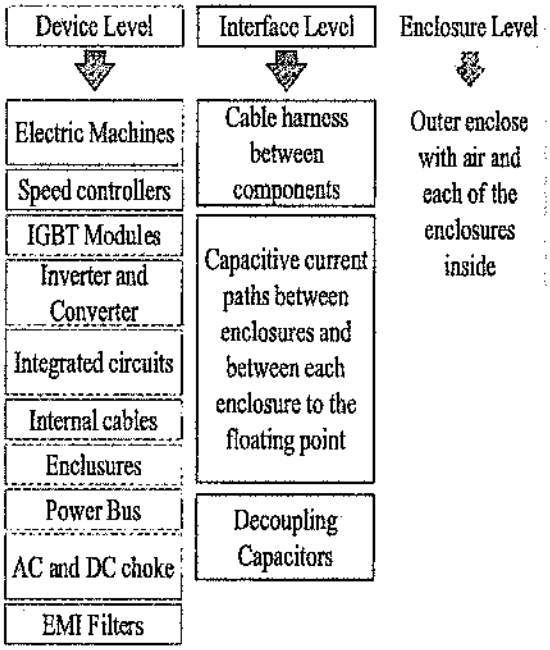

Fig. 1. Decomposition of modeling problem for creation of numerical test environment.

B. Numerical virtual prototyping

As previously explained, the modeling problem can be decomposed into three different levels; i.e., device level, interface level, and the environmental level. In each level, the sets of numerical analyses are required to enable the designer to predict the performance measure of the device under developed, either under fault or no-fault situations. Figure 2 illustrates the modeling procedure required at each level to provide the designer with a performance measure.

A schematic view of a complete motor drive system [8,9] is shown in Fig. 3. In this system, the motor component, the Insulated-Gate Bipolar Transistor (IGBT) switch module component, DC bus component, cable component, and the logic components establish the main parts of this system. Each of the components is enclosed in an enclosure, and all of the enclosures are placed inside a chamber that is electromagnetically isolated from outer environment.

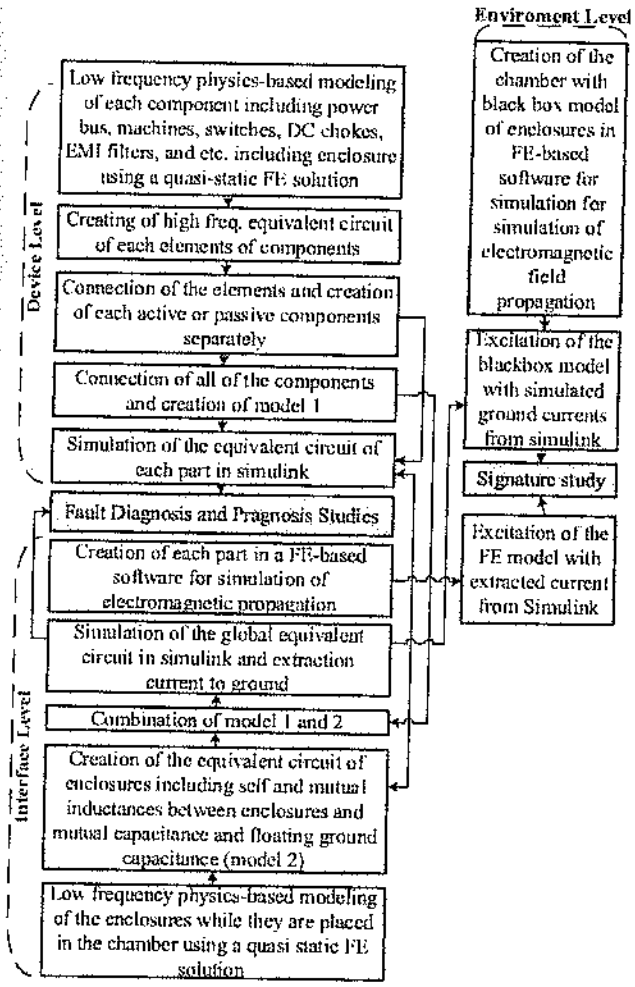

Fig. 2. Functional model of the numerical test environment.

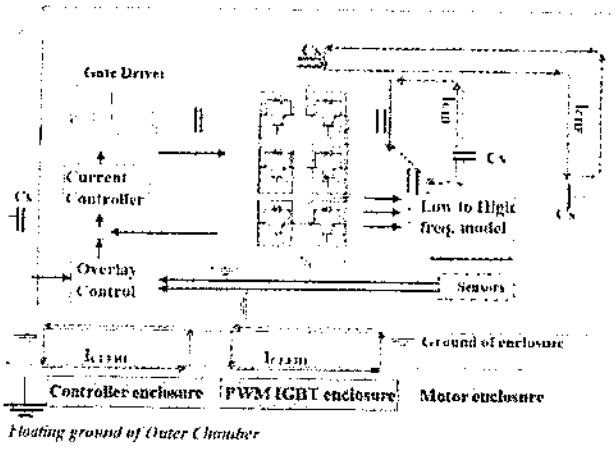

Fig. 3. A view of the numerical test environment for machine-drive design. C_s: stray capacitance, I_{CHF}: high frequency circulating current, I_{CLFHF}: low and high frequency circulating current.

For preparation of the numerical test environment for a motor-drive schema, the following procedure is implemented to evaluate the EMC and EMI in the environment that the motor-drive is located inside. In brief, the step by step implementation of the modeling procedure is summarized as:

1- A coupled field-circuit 3D finite element electromagnetic and electrostatic analysis is done to calculate low to high frequency model of each of the components. For the motor, this task is done both for differential mode and for common mode. This stage is done by using 3D finite element analysis for a given full and equivalent configuration including layout and ground schemes. At this stage, the estimation of the low to high frequency current paths inside the structure of each of the components is also done.

2- Estimation of the current multi-paths between the enclosures, and between each of enclosures to the outer chamber including physically grounded paths and high frequency capacitive paths. Here, the proximity effects, and skin effects are ignored and the static capacitances are calculated; however, the geometry and material effects are taken into account. In the cable component, the enclosure is assumed as the shield of the cable which is grounded.

3- Simulation of the whole motor-drive circuit including all the high-frequency parasitic parameters and extraction of the ground current to the floating ground point from all of the high frequency ground paths and the physically grounded paths in hybrid finite element/circuit modeling.

4- Implementation of the estimated current distributions path inside each of the components via line wires in a 3D finite element software and evaluation of radiated field to the surrounding environment while the simulated line and line to ground current form circuit is modeled as a current source to inject the current to the corresponding line wires that represent the current paths model. At this stage, the FE analysis is limited to the component and its enclosure.

5- Implementation of the estimated current distribution paths via line wires inside the outer chamber along with the enclosures

model, in a 3D finite element software, and evaluation of radiated field to the surrounding environment while the simulated ground currents form circuit model are assumed as current sources that inject the proper current to the their corresponding line wires that represent the current path models.

6- The uncertain and stochastic impact of noise currents propagated by fields can be analyzed through placing a current source noise inside the model.

Through this type of modeling, the complexity of the physics based modeling is split into three shown major sub-problems.

III. EQUIVALENT SOURCE MODELING

In this section, the electromagnetic signature study of electrical components is estimated by evaluating the fields at a distance from their sources. A numerical three-dimensional model is developed and utilized for this purpose. The estimation of these radiated fields from electrical components requires significant computational time, especially for cases involving multiple components such as generators, motors, power converters and cable-run (see Fig. 4).

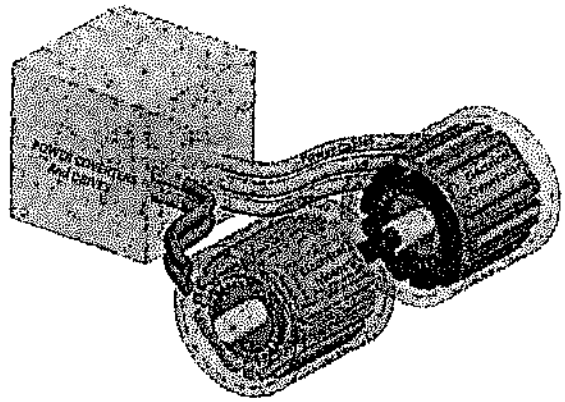

Fig. 4. Prototype of a multi-component system.

A. Electrical machines

It's proposed to develop equivalent source models using edge modeling technique in finite element analysis to overcome this limitation while maintaining accuracy. The proposed model consists of loops with various branch currents and node voltages as shown in Fig. 5 [8-10].

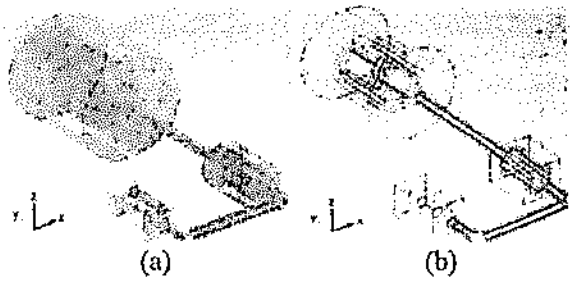

Fig. 5. Schematics of the power setup: (a) full FE model, and (b) equivalent model.

In order to model a multi component system in a large study environment, each of the components need to be modeled individually (see Fig. 5). The wire model of the system is designed and created based on the current directions. The path of the winding arrangement for the machine and the other components, including the position of the voltage terminals, should be identified. The models are shown in Figs. 5 (a) and (b). As shown in this figure, the wire model consists of numerous lines with specific currents flowing and voltages established at the nodes of these wires. The currents of the wire model are calculated based on equalizing the magnetic field densities. Using the Biot-Savart law, the radiated magnetic field density of a line at an R distance away from the line is as follows:

$$B_l = \frac{\mu_0}{4\pi}\int \frac{I_l dl \times \hat{a}_R}{R^2}, \tag{1}$$

where the l is the length of the line and I_l is the carrying current of the line and $\hat{a}_R$ is the unit distance vector between dl and the observation point. Similarly, for a volume current, the radiated magnetic field density at a distance R is as follows:

$$B_v = \frac{\mu_0}{4\pi}\int \frac{J dv \times \hat{a}_R}{R^2}. \tag{2}$$

The idea of this model is to have the same field, while the model is a line and doesn't have cross-section. Hence, by equalizing the two above equations and considering J, R, ds and dl as the known parameters, then the I_l, the current amplitude of the line, can be calculated. The voltages of nodes are similarly calculated by equalizing the electric field due to the charge distribution of the line and the volume. More

details about the basics of the model are mentioned in [10].

The magnetic fluxes radiated from the actual and the wire models are derived from the simulation at 7 m away from the arrangement and shown in Figs. 6 (a) and (b), respectively. As can be seen, the magnitude of the radiated magnetic field of the optimized wire model is almost the same as the full 3D model. The proposed wire model performed the analysis accurately while the analysis time was significantly shorter in comparison with the full 3DFE model (about 50 times lower), while the full model had 8 million degrees of freedom versus one million degrees of freedom of the equivalent model.

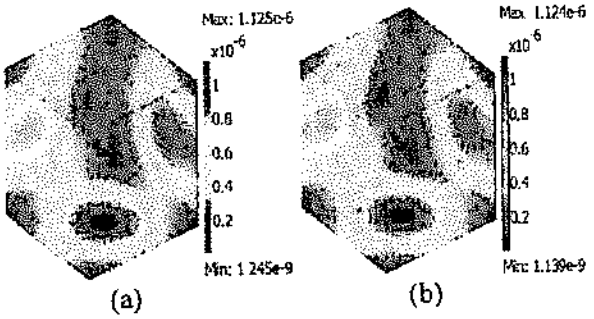

(a) (b)

Fig. 6. Radiated magnetic flux density of: (a) 3D full model, and (b) wire model in Tesla (T).

The simulated model is verified experimentally based on the setup shown in Fig. 7. The setup consists of a synchronous generator: 13.8 kW, 3 phase, 230 V; induction motor: 3 phase, 5.5 kW, 230 V; 3 kW AC load, XLPE cable with armored PVC sheathed. The coil antenna and the real-time spectrum analyzer which is used in the measurement are specifically for low frequency analysis with high precision. The frequency range is between 20 Hz-500 kHz. The winding of the antenna is 36 turns of 7-41 litz wire shielded with 10-Ohms resistance and 340 μH inductance. The antenna and the setup are located based on the standards (MIL-461-STD). The spectrum analyzer, also covers 1 Hz - 3 GHz with ±0.5 dB absolute amplitude accuracy to 3 GHz. Note that there is a controller connected to the drive shown in Fig. 7 which is out of the system and the system is turned on manually.

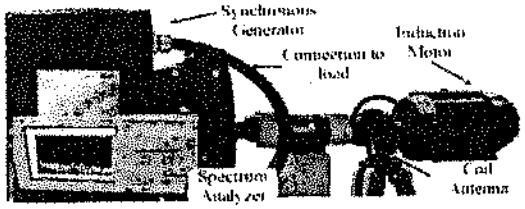

Fig. 7. The studied setup including machines, measurement equipment and control drive (for switching).

As the case study, all components including the synchronous generator, the induction motor and the electric load are turned on. The cables are passing currents; therefore, they also can be considered ON. All switches are turned on and the H-field is measured experimentally and also obtained from the simulation models. The machines are tested at their nominal voltages. The magnetic field intensity (H-field) of the measurement and simulation models is shown in Fig. 8. As shown in this figure, the full finite element model and the wire model have similar radiated H-field compared to the measurement. The small differences of the amplitudes are because of the effects of the bodies of the other components around the system.

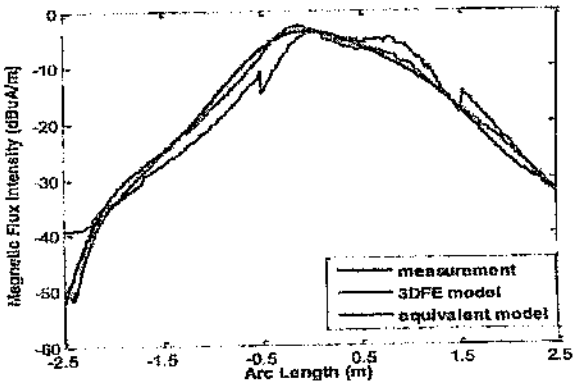

Fig. 8. The measured magnetic field intensity at 55 cm far from the setup on Y axis while all components were turned on at 60 Hz (dBμA/m).

The informative part of the figure for the monitoring purpose is the peak point at the critical frequencies, such as the power frequency and the consequent harmonics. Since the machines are

designed to be symmetric, the peak of the radiated H-field would be placed on a perpendicular line in the lateral side of the motor's casing at equal distance from the two sides of the shaft (see the dashed line in Fig. 9). This can be inferred by comparing Fig. 8 and Fig. 10. Hence, if the peak point of the Fig. 8, which is located at the junction of the dashed line and the solid line, moves back or forward along the solid line in Fig. 9, then this shift may be considered as a symptom of the asymmetry or unbalanced condition of the motor.

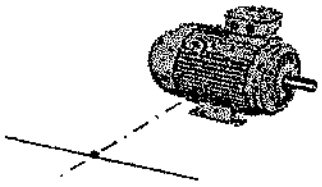

Fig. 9. The assumed line perpendicular to the lateral side of the motor. The maximum field is radiated at this point.

The frequency response of the experimental setup is also shown in Fig. 10 for both switch cases. Comparing Fig. 10 (b) with Fig. 10 (a), since there are two 4pole machines running in this case, the peak at the mechanical frequency which is 30 Hz, has higher amplitude at 55 cm away from the setup. For recognition of the operating machines, this can be considered as a helpful symptom. Note that, the peak of the H-field at 60 Hz in Fig. 10 (a) is the effect of the other components in the vicinity of the setup arrangement [11].

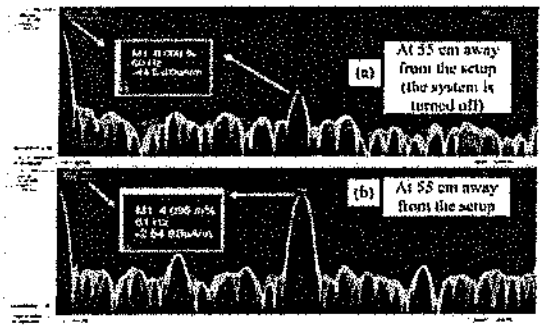

Fig. 10. The measured magnetic field intensity at distance away from the setup in lateral side of the motor while all components except IM were turned off (dBμA/m). The bandwidth of frequency is 120 Hz and the center frequency is 60 Hz.

B. Power converters

The same procedure of modeling is applied for the power converter with the exception that the power electronics converter has switches and the switching activities should be considered. The prototype of the inverter's FE model is shown in Fig. 11.

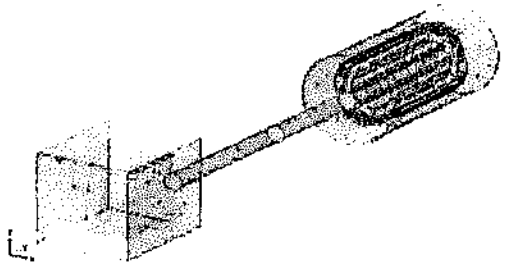

Fig. 11. The prototype of the inverter, induction motor and the connection cable.

To model the IGBT switches of the inverter for signature studies, the switches must be considered OFF for a moment of time and then it must be considered ON for the next time instant. This shift occurs based on the switching frequency of the converter. In order to do this in FE simulation, the plate between the load and the positive bus, shown in Fig. 12, is considered a conductive plate for the switch-ON case. Subsequently, this plate is considered a non-conductive plate for the switch-OFF case. This alteration of the conductivity of the plate occurs 5000 times in a second due to the switching frequency (5 kHz).

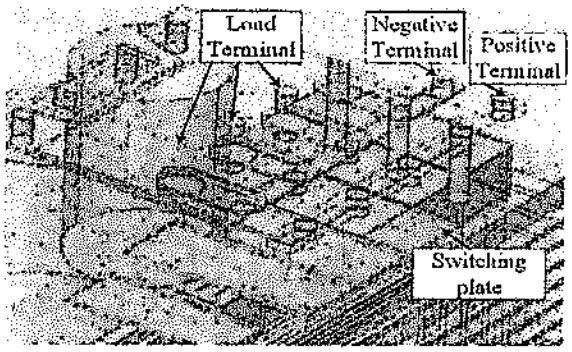

Fig. 12. Physical model of the inverter switches.

The simulation was computed in six hours with about one million elements including face,

line and node meshes in the model with six million degrees of freedom. The large number of elements is necessary because of the very small surfaces, edges and lines of the critical part of inverter and cable, as shown in Fig. 13. The details of FE modeling is reflected in [12]-[14]. The simulation was performed in a fast computer with 192 GB RAM and 16 core Intel Xeon 3.47 GHz CPU.

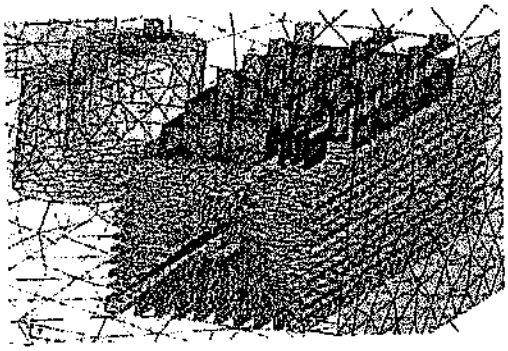

Fig. 13. Mesh pattern of the modeled inverter.

As the case study, the inverter is connected to an induction motor. The induction motor is the same as the previous test. The inverter is 5.5 kW, 320 V, 3 phase with space vector modulation as the switching algorithm. The simulation was computed in six hours with 950,000 elements and 5.7 million degrees of freedom (one million mesh elements). Since the case includes very small elements and also nonlinear materials, e.g., the core of the machine, the simulation of the inverter connected to the load or motor may take 8 hours or more for only one time instant. The experimental setup is shown in Fig. 14.

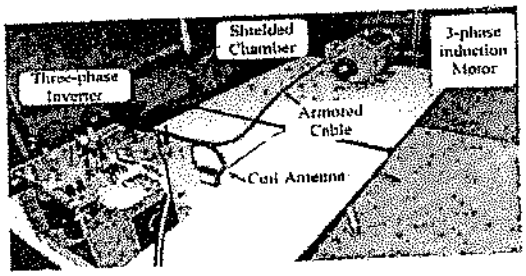

Fig. 14. The scheme of the measurement setup shown in Fig. 11.

Generally, linear or non-linear solvers are being used in the FE simulations. In this case, since there are several materials with nonlinear characteristics, the linear solver cannot be used. On the other hand, using nonlinear material rises the simulation time dramatically. Hence, a modified solver and an associated iterative technique was employed. Instead of having linear or curved commutation curve, the ramp of the curve in several zones was calculated (μ_{r1}, μ_{r2} ...) and used instead of the commutation curve in this part as shown in Fig. 15. The benefit of this modification is that the magnetic flux density of a component changes in a very small period due to the steady state condition of the system. For example, the magnetic flux density of the stator core of the induction motor is about 1.5-2 T in power frequency analysis, 50-60 Hz. For higher frequencies, it goes down to under 1 T. Therefore in this case, a specific zone of the permeability can be chosen for this component. Similarly, the permeability of the other components of the system can be chosen based on the working frequency. Therefore, having the idle parts of the commutation curves of the elements would be avoided and the simulation time decreases. This algorithm can be applied in the material defining part of the FE simulation.

In addition to the modification in defining the material properties, some modification needs to be performed for the solver to have a flexible solution. Hence, as the iterative solver, the fast Generalized Minimal Residual Technique (GMRES), with the Krylov as the pre-conditioner was used. The fast GMRES is a variant of the GMRES method with flexible preconditioning that enables the use of a different pre-conditioner at each step of the Arnoldi process. The Krylov subspace is a linear subspace which enables multi-preconditioning [15]. In particular, a few steps of GMRES can be used as a pre-conditioner for fast GMRES. The flexibility of this solution method is beneficial for the problem with nonlinear material characteristics such as the motor's core. Therefore, the simulation time decreases from about 8-9 hours to about 20 minutes. More explanation is given in [16].

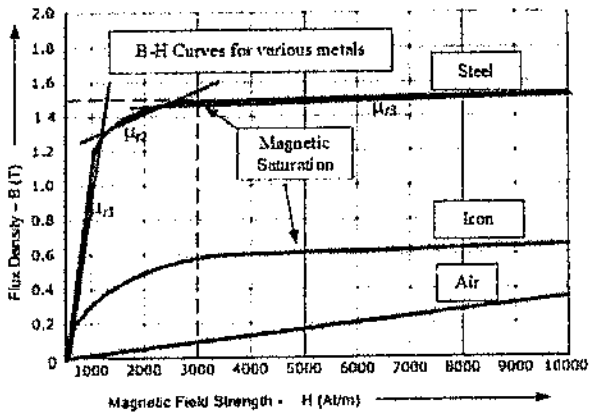

Fig. 15. Magnetization curves of some material used in the simulation.

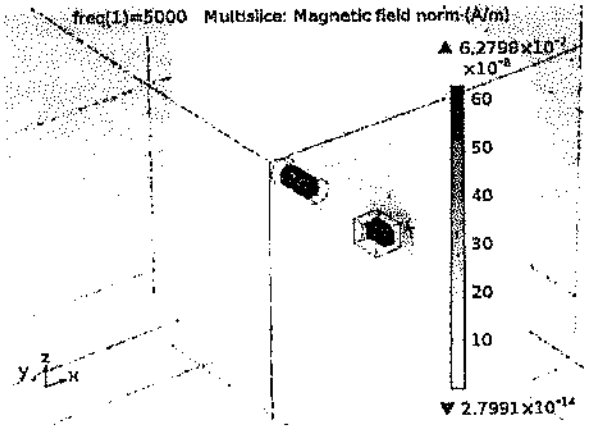

Fig. 16. Stray magnetic field intensity of the setup case 2 at 5 kHz simulated in FE (μA/m).

In addition to the simulation, the experimental setup was implemented in a chamber which isolates the setup from the outside environment, shown in Fig. 14. The coil antenna was located at 10 cm away from the inverter to obtain the stray magnetic field. The fields were transferred to an EMI receiver, real-time spectrum analyzer, with a cable of 50-Ω impedance.

The magnetic field intensity (H-field) generated from the setup in simulation is shown in Fig. 16. The H-field at 5-kHz frequency is shown on a slice at 10 cm away from the setup, the same as experimental setup. As illustrated in this figure, the amplitude of the stray field around the inverter box is higher than other places. The reason is that the switching frequency of the inverter is 5 kHz, the same as the frequency depicted from the simulation figure. The simulation was performed at several other frequencies. Only the switching frequency of the inverter which is 5-kHz, is shown here. The setup was also implemented experimentally. The frequency response from DC to 20-kHz was obtained and shown in Fig. 17.

The unit of the simulation result is μA/m, while the unit of the experimental results is dBμA/m. The μA/m can be converted to dBμA/m by using Eq. (3). Using this equation, the peak of the stray magnetic field at 5-kHz at the given distance is -4.37 dBμA/m would be 0.61 μA/m experimentally, which is very close to the value in simulation, see Fig. 16;

$$\mu A/m = 10^{\frac{dB\mu A/m}{20}}. \quad (3)$$

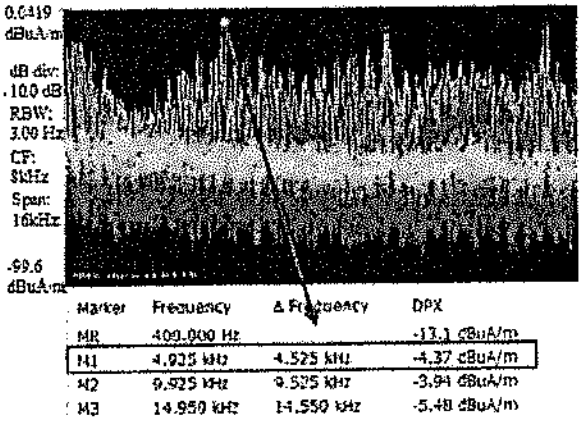

Fig. 17. Measured frequency response of the stray magnetic field intensity of the setup from DC to 20 kHz (dBμA/m).

C. Power cables

The actual physical modeling of cables for signature studies requires all the details to be considered even in a large region. The XPLE cables similar to all electromagnetic sources propagate dipoles at a far distance. However, interacting several components such as electrical machines, power converters modify the shape and the amplitude of dipoles. Therefore, each model should be modeled and studied independently. However, there is a problem with the modeling of the relatively small layers of a multi-core XLPE cables. The study region could be about 20,000 times bigger. This causes deformation of the cable's model during meshing in numerical

modeling method. The present study is performed on the XLPE insulated and armored PVC sheathed cable (0.6/1 kV).

Figure 18 shows the typical model, as well as original and the deformed models of the studied cable in finite element analysis environment. In order to solve this issue, a specific modeling including multi dipoles with several line currents and node voltages are designed similar to the procedure explained in III.A. As shown in Fig. 19, the model is replaced by a collection of lines located in the position of the windings in actual machine. More details are mentioned in [17].

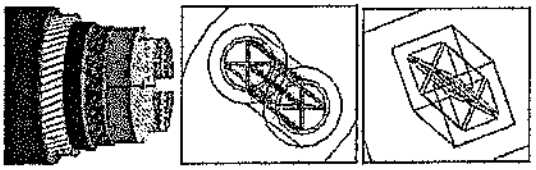

Fig. 18. Models of the proposed cable in finite element design: (a) typical model, (b) orignial FE model, and (c) deformed FE model.

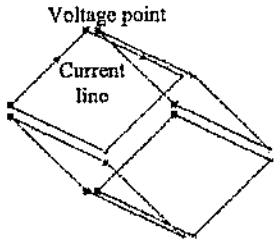

Fig. 19. Prototype of the multi-dipole models of the studied cable.

Many case studies are implemented related to cables, but for brevity only one of them is explained in the following.

The proposed model is analyzed in connection with a power component. A synchronous generator is coupled with a multi-core XLPE cable. In order to model the synchronous generator, the wire modeling is used which is basically similar to the proposed modeling of the cable, further details are explained in [18]. The actual and equivalent models of the cable connected to the machine are shown in Fig. 20.

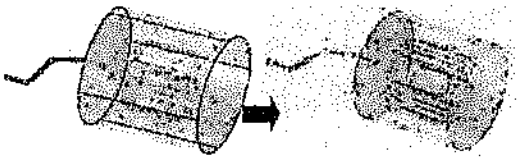

Fig. 20. Schematic of the synchronous machine connected to the cable: (a) the detailed model, and (b) the equivalent model.

The rated voltage is applied to the cable which is connected to the machine and the radiated field is measured at a far distance from the sources. Also, the current and voltage values of the equivalent model are calculated based on the individual actual models of the machine and cable. Figure 21 shows the propagated fields of both models along X axis in XY plane. The proposed line is also shown in the figure. The difference of amplitude between these two models is because of superposition of materials. Since the cables and machine are so close together, therefore, there is a superposition effect in magnetic field. The radiated magnetic field from cable is induced into the machine and creates an induced current which radiates an additional field from the machine. These phenomena cannot be simulated perfectly in the proposed multi-dipole modeling so there is a difference in the curves. More studies are in [17].

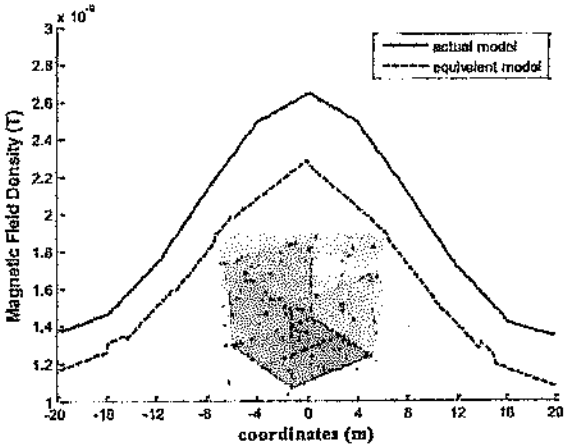

Fig. 21. Radiated magnetic field density along X axis in XY plane.

IV. HIGH-FREQUENCY EQUAIVALENT SOURCE MODELING

For EMC modeling the power components, especially power electronic components such as drives and converters, the high frequency modeling of them is needed which is implemented based on Fig. 22. The detail models of the power converters are reflected in [19].

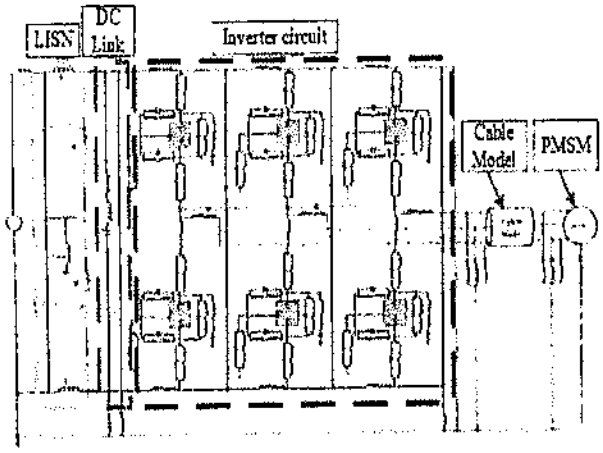

Fig. 22. Inverter circuit of AC motor drive, used in simulation with inclusion of parasitic components.

Figure 23 demonstrates the connection of a three-phase 42-V inverter, armored power cable and three-phase PMSM. The inverter adopts power IGBT as the switching device. In the inverter model, all the semiconductor devices are substituted with their corresponding physics-based models. To simulate such an inverter drive, the time-domain simulation approach is used. To construct the simulation model for motor-drive system, the three major components of the system (i.e., inverter, cable and PMSM) are replaced with their corresponding physics-based models.

The test setup used to measure the frequency spectrum in different point in the drive system is shown in Fig. 23 (b). The illustrated test setup consists of a DC power supply, LISN, inverter circuit, 2 m long armored power cable and a 250 Watt PMSM. To measure the common mode current, all these components are assembled on a metallic plate. Subsequently, the conducted current can be measured between these plates. In order to avoid time-consuming computing process and better evaluation, the frequency domain simulation approach is used.

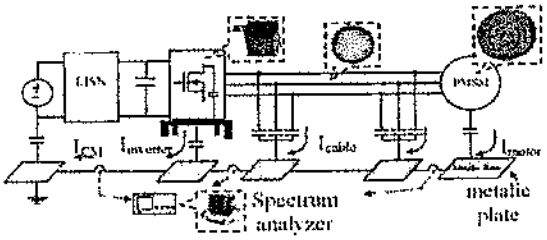

(a)

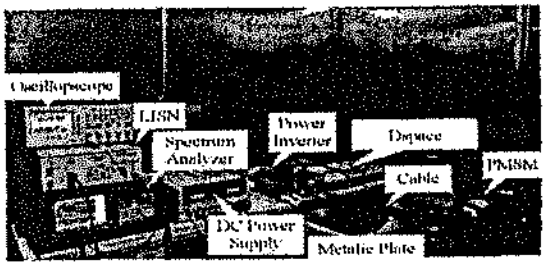

(b)

Fig. 23. Schematic view of a motor-drive system: (a) schematic of motor-drive system used for CM measurement, and (b) experimental setup.

Figure 24 shows the system structure in the FE model. This model was solved to estimate the values of the parasitic elements in the circuit model. Figure 25 shows comparisons of conducted EMI common mode between the measurements data and two modeling approaches in the frequency domain.

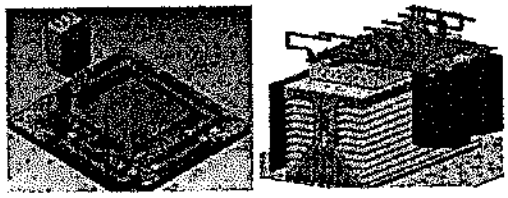

Fig. 24. The converter model in finite element and its corresponding mesh.

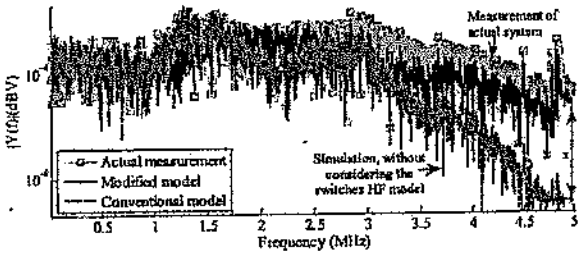

Fig. 25. Frequency spectrum of the common mode current.

To study the effectiveness of our models, the equivalent models for cable and PMSM were added to the inverter model and the simulation results are compared to the experimental results. To verify the accuracy of our numerical results, the common mode current of the setup in Fig. 24 was measured using the current probe with 100 MHz bandwidth. The current of Fig. 24 is measured at the ground port of the input DC power supply.

As an application of this modeling, three switching techniques (Hysteresis, Space Vector Modulation and Sinusoidal PWM) with a carrier frequency of 5 kHz applied to the inverter. A three-phase 5 kW RL load was connected to the inverter, which makes the inverter operate at nominal power. The calculated currents were then injected to the terminals in the 3D-FE based model. The 3D-FE solution was obtained using harmonic propagation analysis. The step time for this simulation was 5 μs. To validate the obtained numerical results, the experimental setup was implemented and the inverter's phase current spectrum is measured using a spectrum analyzer and a 100 MHz current probe. The measured and simulated frequency spectrums of the inverter's phase current for SVM as an example is shown in Fig. 26. Subsequently, the magnetic field spectrum of the components designed using the physics based modeling are shown in Fig. 27.

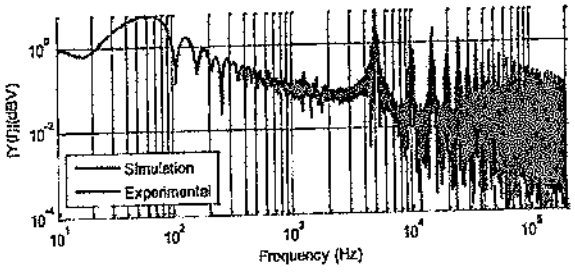

Fig. 26. Comparison of the frequency spectrum of the inverter's phase current between equivalent model and experiments.

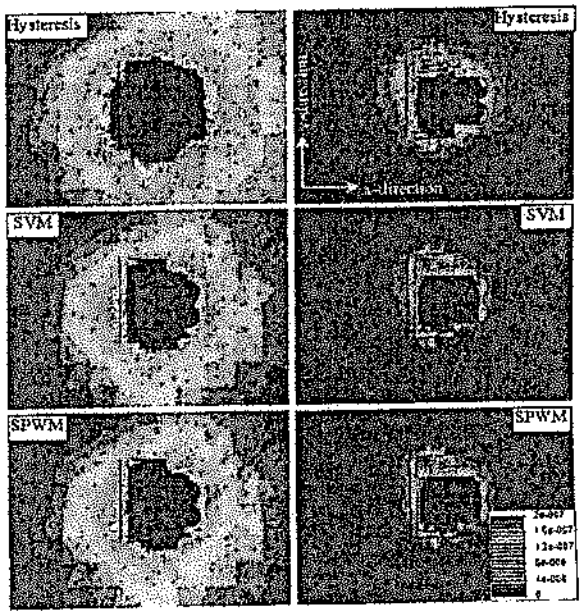

Fig. 27. Magnetic flux density at different switching patterns before (left) and during switching (right): (a) hysteresis, (b) SVM, and (c) SPWM.

It can be easily inferred from the figure that within this model, various parameters can be changed and studied in order to identify an EMI mitigation strategy during the design stage of these systems. In the proposed model, the EMI can be analyzed at any point or plane within the simulation volume, and can be solved for different switching patterns. The time dependence of the radiated EMI can also be evaluated using the model. We can see how the magnetic flux density behaves over time at specific locations and at various switching patterns and frequencies. Furthermore, the field image can be obtained for various scenarios specified by the designer and provide them with information that can be obtained quickly. This would allow for efficient and effective complete design work using computational electromagnetics.

V. OPTIMIZATION OF POWER ELECTRONIC CONVERTERS USING PHYSICS-BASED MODELS

In this study, the optimization of a physics-based representation of a frequency modulated switch mode converter is presented. The proposed physics based model can be used to evaluate the electromagnetic interference in the structure of the converter. In this method, the power converter magnetic components and their position on the circuit board are modeled numerically using Finite Element Analysis (FEA). Subsequently, the placement of the components and also the electrical and operating parameters of the converter are optimized in a way to limit the propagated electromagnetic field of the components. This is an essential fact in design of the power converters and the evaluation of their EMI interactions for EMC compliance.

Figure 28 depicts the flowchart of the parameter optimizing procedure using GA. Parameters for optimization are the converter's operating parameters and placement of the magnetic components with respect to each other. The genetic algorithm evolves the given population of individuals. The object function is consisting of the area of the circuit board and energy of the output voltage signal. In order to change the area which confines the two inductors, the filter inductor's position is considered as a reference and the resonant inductor placement is changing all around the reference point (filter inductor). Figure 29 illustrates the process of changing the placement of the two inductors as with respect to each other.

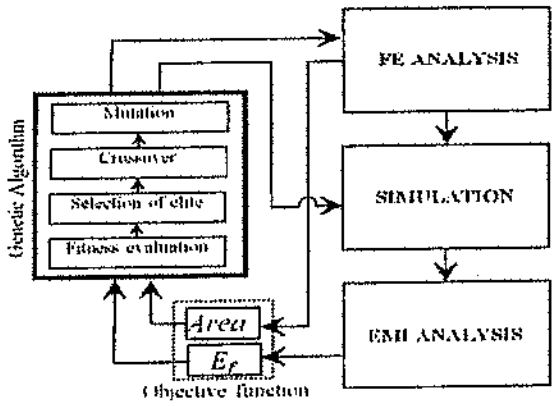

Fig. 28. The optimization process diagram.

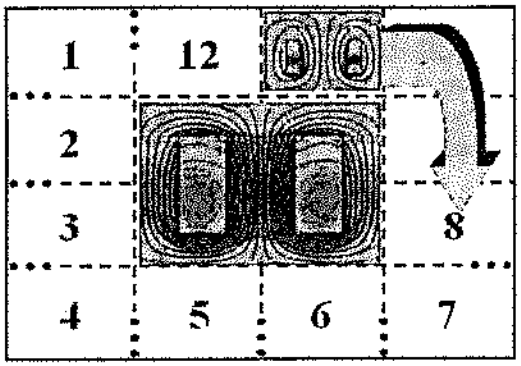

Fig. 29. Iteration accomplished by GA to minimize the objective function.

Table 2 shows the results from the optimization process. The magnetic component positions of this converter are shown in Fig. 30. It is clear that this power converter is showing a poor EMI performance at initial design stage (Fig. 29 (a)). FE analysis is performed observe the near-field effects for the given layout. Further, we performed repeated simulations to determine the best EMI performance versus geometry of the board and the frequency (Fig. 30 (b)).

Table 2: Optimization results

Parameters	L_r (μH)	f (kHz)	Area (mm^2)
Initial design	120	50	3360
Optimized design	45	90	11000

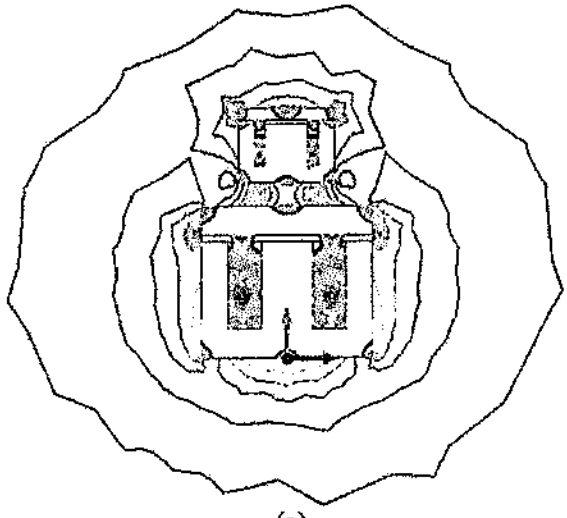

(a)

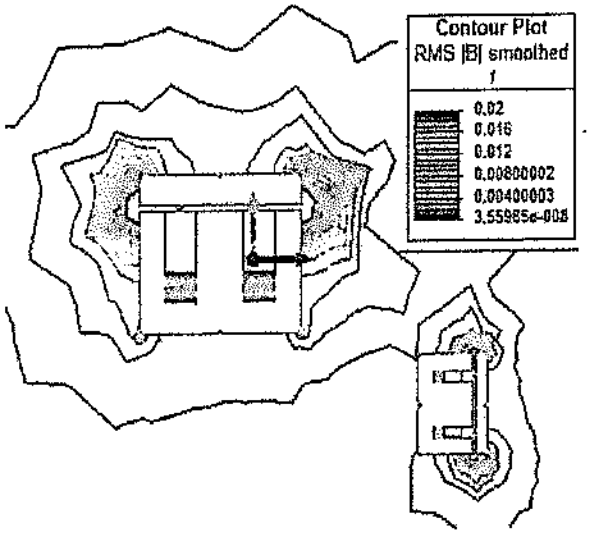

(b)

Fig. 30. Layout of the system: (a) before optimization, and (b) after optimization.

Figure 31 compares the input current spectrum, filter inductor's current spectrum and output voltage spectrum of the converter in the ideal case and physics-based mode (non-optimized case), respectively. It is noticed that in the optimized case, the pick of the frequency spectrum has been decreased, as compared to the non-optimized case. Figure 32 shows the circuit layout of the converter in the optimized case. In this case, the magnetic components are placed, somehow, that the magnetic field generated by each one has the less interference with the other. More details are reflected in [20].

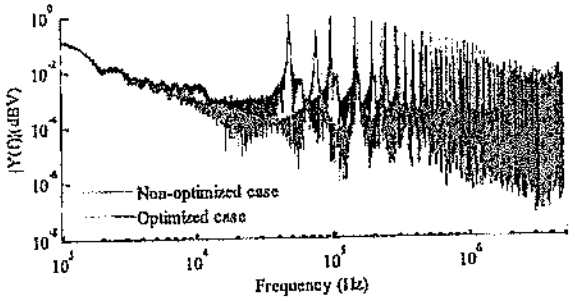

Fig. 31. Comparison of FFT spectrum between optimized and non-optimized quasi-resonant converter, resonant inductor's current.

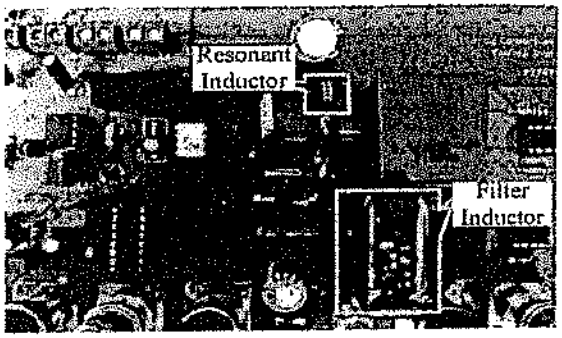

Fig. 32. ZCS quasi-resonant buck converter's circuit in the optimized layout.

VI. CONCLUSION

This paper reviewed the physics based modeling analysis for the purpose of EMC evaluation in multi components power system. It introduced the algorithm of physics based modulation for both low and high frequency analysis. The equivalent source modeling of the powertrain was implemented for EMC studies and the results showed that the equivalent model can make the same result of the full model with significantly less simulation time. The model has been used for condition monitoring of the components based on the EM signatures. Moreover, the optimization of the switching algorithm, as well as the proper placement of the magnetic components on the PCB was achieved all based on the radiated electromagnetic fields.

AKNOWLEDGEMWNTS

Part of this work was supported by a grant from the Office of Naval Research.

REFERENCES

[1] W. Zhang, M. T. Zhang, F. C. Lee, J. Roudet, and E. Clavel, "Conducted EMI analysis of a boost PFC circuit," *IEEE Appl. Power Electron. Conf.*, pp. 223-229, 1997.

[2] B. Revol, et al., "EMI study of a three phase inverter-fed motor drives," *IEEE Industry Applications Conference, 2004*, vol. 4. IEEE, 2004.

[3] Y. L. Zhong, et al., "HF circuit model of conducted EMI of ground net based on PEEC," *Zhongguo Dianji Gongcheng Xuebao*, vol. 25, no. 17, 2005.

[4] H. Zhu, et al., "Analysis of conducted EMI emissions from PWM inverter based on empirical models and comparative experiments," *IEEE*

Annual Power Electronics Specialists Conference, (PESC 99), 30th, vol. 2, 1999.

[5] X. Pei, et al., "Analytical estimation of common mode conducted EMI in PWM inverter," *IEEE Industry Applications Conference*, vol. 4, 2004.

[6] L. Sevgi, "EMC and BEM engineering education: physics-based modeling, hands-on training, and challenges," *IEEE Antennas and Propagation Magazine*, vol. 45, no. 2, pp. 114-119, 2003.

[7] D. S. Dixon, M. Obara, and N. Schade, "Finite-element analysis (FEA) as an EMC prediction tool," *IEEE Transactions on Electromagnetic Compatibility*, vol. 35, no. 2, pp. 241-248, 1993.

[8] A. Sarikhani, M. Barzegaran, and O. A. Mohammed, "Optimum equivalent models of multi-source systems for the study of electromagnetic signatures and radiated emissions from electric drives," *IEEE Transaction on Magnetics*, vol. 48, issue 2, pp. 1011-1014, 2012.

[9] M. R Barzegaran, A. Sarikhani, O. A. Mohammed, "An optimized equivalent source modeling for the evaluation of time harmonic radiated fields from electrical machines and drives," *Applied Computational Electromagnetics Society Journal*, vol. 28, no. 4, pp. 273-282, April 2013.

[10] M. R Barzegaran and O. A. Mohammed, "A generalized equivalent source model of AC electric machines for numerical electromagnetic field signature studies," *IEEE Transaction on Magnetics*, vol. 48, no. 11, November 2012.

[11] M. R Barzegaran and O. A. Mohammed, "3-D FE equivalent source modeling and analysis of electromagnetic signatures from electric power drive components and systems," *IEEE Transaction on Magnetics*, vol. 49, no. 5, pp. 1937-1940, May 2013.

[12] M. R. Barzegaran, A. Nejadpak, and O. A. Mohammed, "Evaluation of high frequency electromagnetic behavior of planar inductor designs for resonant circuits in switching power converters," *Applied Computational Electromagnetic Society (ACES) Journal*, vol. 26, no. 9, pp. 737-748, September 2011.

[13] G. Skibinski, R. J. Kerkman, and D. Schlegel, "EMI emissions of modern PWM AC drives," *IEEE Ind. Appl. Mag.*, vol. 5, no. 6, pp. 47-80, 1999.

[14] O. Martins, S. Guedon, and Y. Marechal, "A new methodology for early stage magnetic modeling and simulation of complex electronic systems," *IEEE Trans. Magn.*, vol. 48, no. 2, pp. 319-322, 2012.

[15] W. E. Arnoldi, "The principle of minimized iterations in the solution of the matrix eigenvalue problem," *Quarterly of Applied Mathematics*, V. 9, pp. 17-29, 1951.

[16] J. Stoer and R. Bulirsch, "Introduction to numerical analysis," 3rd edition, *Springer*, New York, 2002.

[17] M. R Barzegaran and O. A. Mohammed, "Multi-dipole modeling of XLPE cable for electromagnetic field studies in large power systems," *International Journal for Comp. and Math. in Electrical Eng. (COMPEL)*, vol. 33, no. 1, 2014.

[18] M. R Barzegaran and O. A. Mohammed, "Near field evaluation of electromagnetic signatures from wound rotor synchronous generators using wire modeling in finite element domain," *28th ACES Conf.*, Columbus, OH, USA, April 2012.

[19] A. Nejadpak, "Development of physics-based models and design optimization of power electronic conversion systems," *FIU Electronic Theses and Dissertations*, paper 824, (2013).

[20] A. Nejadpak and O. A. Mohammed, "Physics-based optimization of EMI performance in frequency modulated switch mode power converters," *Electromagnetic Field Problems and Applications (ICEF)*, pp. 1-4, June 19-21, 2012.

Mohammadreza Barzegaran (S'10) obtained his B.Sc. and M.Sc. degrees in Power Engineering from the University of Mazandaran, Iran in 2007 and 2010, respectively. He defended his Ph.D. degree in the department of Electrical and Computer Engineering, Florida International University, Florida, USA. He is now Assistant Professor at Lamar University. His research interests include studying electromagnetic compatibility in power components, life assessment of electrical power components, fault detection in electrical machines, and also computer-aid simulation of power components. He has many published papers in journals and conferences.

Osama A. Mohammed (S'79, M'83 SM'84, F'94) is a Professor of Electrical and Computer Engineering and the Director of the Energy Systems Research Laboratory at Florida International University. He received his M.S. and Ph.D. degrees in Electrical Engineering from Virginia Polytechnic Institute and State University. He published numerous journal articles over the past 30 years in areas relating to power systems, electric machines and drives, computational electromagnetics and in design optimization of

electromagnetic devices, artificial intelligence applications to energy systems. He authored and co-authored more than 350 technical papers in the archival literature. He has conducted research work for government and research laboratories in shipboard power conversion systems and integrated motor drives. He has been successful in obtaining a number of research contracts and grants from industries and Federal government agencies for projects related to these areas. Mohammed also published several book chapters including Chapter 8 on Direct Current Machinery in the Standard Handbook for Electrical Engineers, 15th Edition, McGraw-Hill, 2007 and a book Chapter entitled "Optimal Design of Magnetostatic Devices: The Genetic Algorithm Approach and System Optimization Strategies," in the Book entitled: Electromagnetic Optimization by Genetic Algorithms, John Wiley & Sons, 1999.

Mohammed is a Fellow of IEEE and is the recipient of the IEEE PES 2010 Cyril Veinott Electromechanical Energy Conversion Award. Mohammed is also a Fellow of the Applied Computational Electromagnetic Society. He is Editor of IEEE Transactions on Energy Conversion, IEEE Transactions on Magnetics, IEEE Transactions on Smart Grid and COMPEL. Mohammed was the past President of the Applied Computational Electromagnetic Society (ACES). He received many awards for excellence in research, teaching and service to the profession and has delivered numerous invited lectures at scientific organizations around the world.

Mohammed has been the General Chair of several international conferences including ACES-2013, ACES 2006, IEEE-CEFC 2006, IEEE-IEMDC 2009, IEEE-ISAP 1996 and COMPUMAG-1993. He has also Chaired technical programs for other major international conferences including IEEE-CEFC 2010, IEEE-CEFC-2000 and the 2004 IEEE Nanoscale Devices and System Integration. Mohammed also organized and taught many short courses on power systems, electromagnetics and intelligent systems in the U.S.A and abroad.